Deformations in Cold-bent HSS Members

JOHN B. KENNEDY, MOKHTAR SEDDEIK AND FRANK BRADY

ABSTRACT

The purpose of this investigation is to predict the relation between the radius of bend and the distortion of Hollow Structural Section (HSS) members. An experimental program was carried out using twenty-seven different profiles of HSS members. The pyramid-type, three-roller bending machine was used as the method of cold-bending. The cross-section distortion is defined by two parameters that describe the permanent deformations in the flange and web of the cross-section. Multiple regression analysis was used to obtain a relation between each of these parameters, the cross-section properties and the radius of bend. The effect of the resulting distortion on the moment of inertia of the HSS member is also studied. A parametric study is undertaken to demonstrate the influence of the change in the cross-section dimensions on the permanent distortion.

MANY POTENTIAL APPLICATIONS

Curved Hollow Structural Section (HSS) members of square and rectangular geometry have many potential applications in the field of structural engineering. The permanent curvature of such members is effected by special rolling machines. In the present study, cold-bending of HSS members with the pyramid-type rolling machine is used. When compared to other methods of bending, this method was available, economical and most suitable for the large radii of bend required for construction purposes. Because of the cost involved, no considerations were given to heating the members prior to bending or to packing them with any type of filler material.[2]

During the cold-bending process, the relatively thin component plates of the HSS member are subjected to large deformations causing permanent distortion of the cross-section. The magnitude of such deformations depends on the cross-section dimensions, material properties as well as on the radius of bend imposed on the member. To establish a relation between these variables, an experimental program was carried out on 27 different sizes of HSS beam specimens. All tests were conducted at Hodgson's Steel and Iron Works in Niagara Falls, ON, Can.

John B. Kennedy is professor of Civil Engineering, University of Windsor, Windsor, Ontario, Canada.
Mokhtar Seddeik is research assistant in Civil Engineering, University of Windsor, Windsor, Ontario, Canada.
Frank Brady is engineer in charge, IEC-Holden Inc., Montreal, Quebec, Canada.

TEST PROGRAM

Specimen Details

A series of 54 tests were carried out on 27 different sizes of square and rectangular HSS members. Two specimens, each 8 ft-2 in. long, were tested from each size. The profiles tested varied from 4.0 × 2.0 × 0.1500 in. to 10.0 × 10.0 × 0.3,750 in. All materials conformed to CSA standard G40.21, Gr. 50, class H. These specifications call for a minimum yield strength of 50 ksi, a tensile strength in the range of 65 ksi to 90 ksi and minimum elongation of 22% in 2-in. length. Sizes up to 24.0 in. in circumference were produced by a continuous weld process, while larger sizes were produced by electric resistance weld process and subsequently stress relieved.

Machine Description

The pyramid-type rolling machine consists of three rollers. The arrangement of these rollers is shown in Fig. 1. Rollers No. 1 and No. 2 are immovable while roller No. 3, through which the load is applied, is movable in the direction indicated. The rollers are mounted vertically in the machine as in Fig. 2. This arrangement makes the member under rolling analogous to a simple beam with point supports at the immovable rollers, and loaded at its mid-span through the movable roller. A typical test arrangement is shown in Fig. 2. All tests were carried out on two separate machines. Specimens up to and including 6 in. in depth were bent on a

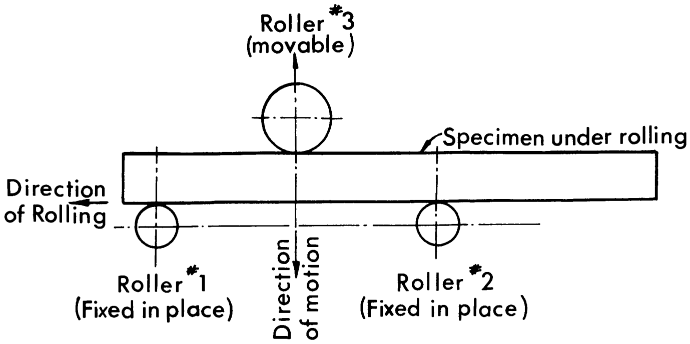

Fig. 1. Set-up of test specimen in a pyramid-type rolling machine (top view)

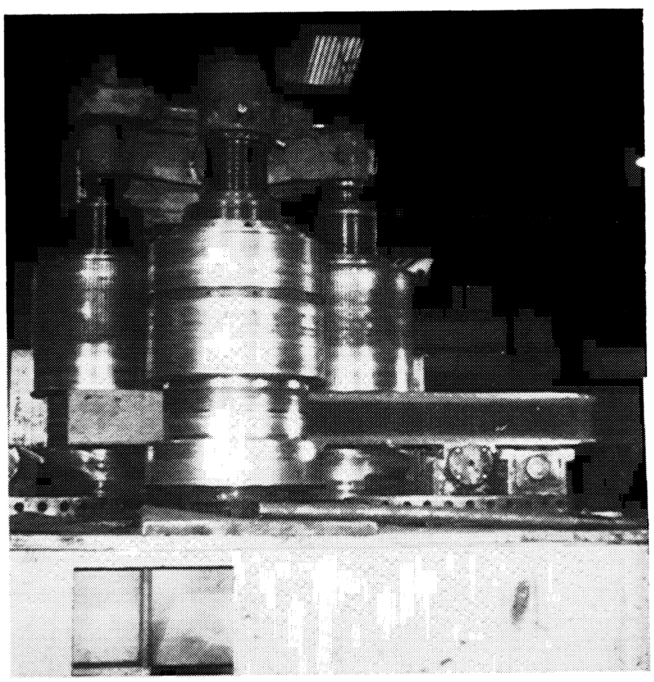

Fig. 2. HSS member in pyramid-type rolling machine

machine with immovable and movable rollers of 15 in. and 17 in. in diameters, respectively. Large size specimens were bent on a second machine with immovable and movable rollers of 18 in. and 20 in. in diameter, respectively.

Testing Procedure

Two identical specimens from each of the 27 chosen profiles were tested. Each specimen was bent to two different radii of curvature, thus providing information about four levels of cross-section distortions. For example, a specimen was bent first to a radius at which minor distortion of the cross-section was apparent. A subsequent length of the specimen was left unrolled; this was followed by a length segment bent tighter until the level of distortion was considered unacceptably large. The specimen was then removed from the machine and accurate measurements of the radius of bend at each length segment of the specimen were made. This rolling procedure was then repeated with the second specimen of the same profile; however, here the values of the imposed radius of bend were intermediate to those measured from the first specimen. Cross-sections were then cut from the length segments bent to each of the four radii and accurate measurements of their dimensions were made.

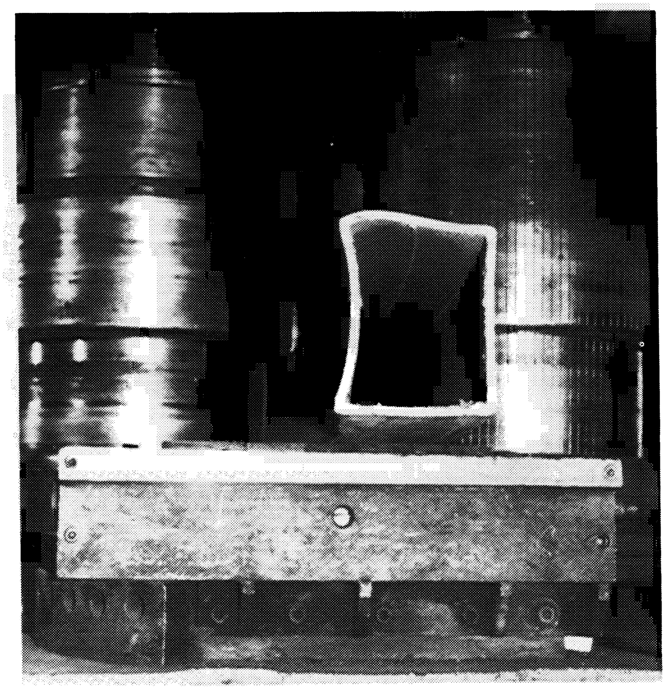

Fig. 3. Distortion in HSS member after rolling

DISCUSSION OF RESULTS

Results from 108 cross-sections (i.e. 4 × 27) representing 27 different HSS sizes studied were analyzed. In all cases the distortions resulting from the rolling process had almost the same pattern, i.e. major permanent deformations in the compression flange (Plate No. 1) and the web (Plate No. 2) facing the top of the rolling machine, while minor distortions resulted in the tension flange (Plate No. 3) and the other web (Plate No. 4) as shown in Fig. 3. The reason for the unsymmetric deformations of the two webs is that the base of the rolling machine acted as a support to one of the webs and thus prevented it from deforming.

Based on the results obtained, two distortion parameters were calculated. Referring to Fig. 4 which shows the dimen-

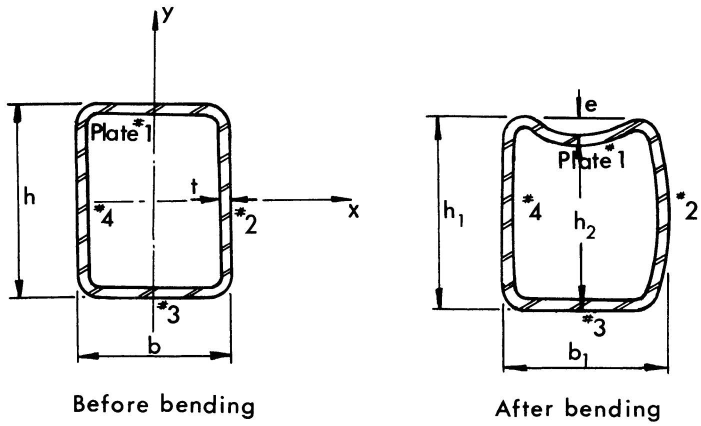

Fig. 4. Rectangular HSS before and after rolling

sions of a cross-section before and after bending, the two parameters are:

1. Percentage increase in width after bending (ρ_b):

$$\rho_b = \frac{b_1 - b}{b} \times 100 \tag{1}$$

2. Percentage bowing in the compression flange after bending (ρ_e):

$$\rho_e = \frac{e}{h} \times 100 \tag{2}$$

where b, b_1, e and h are defined in Fig. 4. The parameters, ρ_b and ρ_e, are listed in Table 1 for the different HSS members tested.

It can be observed that the experimental results presented in Table 1 are spread over a very wide range. Therefore, it was obvious that there is no simple theoretical relationship between the radius of bend and any of the parameters studied. For this reason it was decided to develop such a relationship by using a multiple regression analysis. In the regression equations, the dependent variables were ρ_b and ρ_e while the independent variables were: The radius of bend (R); the dimensions of the undistorted cross-section (h,b,t); and, the moments of inertia (I_x and I_y). Several regression relations were obtained using different combinations of the independent variables. The two relations yielding the highest and statistically significant multiple correlation coefficients were then chosen to describe the two parameters ρ_b and ρ_e.

For the relationship predicting the parameter ρ_b, two model equations gave the same multiple correlation coefficient of 0.86. The first model equation included R, h, b, t, I_x and I_y, while the second included R, h^2/t, h^2/t^2, bh/t, I_x and I_y. The first model equation was finally chosen because of its simplicity. The relationship predicting the parameter ρ_e was best described by a model equation which included R, h, b, t, I_x and I_y. This equation gave a multiple correlation coefficient of 0.90. Therefore, the two chosen regression equations describing ρ_b and ρ_e are:[4]

$$\rho_b\% = (5.074)(R)^{-0.791}\,(h)^{-21.841}\,(b)^{16.367}\,(t)^{-2.737}\,(I_x)^{13.786}\,(I_y)^{-11.362} \tag{3}$$

$$\rho_e\% = (0.339)(R)^{-1.542}\,(h)^{-15.960}\,(b)^{7.416}\,(t)^{-5.609}\,(I_x)^{9.676}\,(I_y)^{-5.462} \tag{4}$$

where R in the radius of bend in meters and all the other variables are in millimeters. The standard errors in Eqs. 3 and 4 were 0.11% and 0.20%, respectively.

It should be mentioned that the experimental test results for the four relatively deep sections with h = 10 in., shown in Table 1, were not used in developing Eqs. 3 and 4; these results were highly inconsistent with the trend of the other results obtained and were proven to be 'outliers'[3]; it is believed these outliers were caused by the frequent adjustments made to the movable roller by the machine operator during the cold-bending process of these deep-sectioned beams; it was observed also that during this process the machine was operating at its maximum capacity.

To test the significance of the multiple correlation coefficient (r) the critical value of r was calculated. Taking the number of observations as 92, i.e. $[(27 - 4) \times 4]$, then for seven variables it was found that the critical value for r = 0.365 at the 1% level of significance.[3] Since the multiple correlation coefficients obtained from the model Eqs. 3 and 4 are much greater than 0.365 the hypothesis that there is no association between the variables is rejected and the deduced relations between the independent and dependent variables can be considered significant. Estimates of the magnitude of the parameters ρ_b and ρ_e from Eqs. 3 and 4 are given in Table 1 for comparison with the experimental results.

It should be noted the uncertainty in the magnitude of the parameters ρ_b and ρ_e depends on the uncertainty of the measurement of each of the independent variables R, h, b, t, I_x and I_y. Based on measurements made on 203 different HSS members, estimates of the coefficient of variation, V, for each of the independent variables h, b, t, I_x and I_y were calculated.[1] These results are shown in Table 2. The uncertainty in measuring R was estimated as 0.1% of the magnitude of the measured value. Applying the theory of error propagation[3] to Eqs. 3 and 4 and using the values given in Table 2, it can be shown that the errors in estimating ρ_b and ρ_e, i.e. (σ_{ρ_b}/ρ_b and σ_{ρ_e}/ρ_e), are 0.072 and 0.294, respectively; since the difference between the uncertainties in the moment of inertia of the rectangular and square sections, is small, the larger values, that of the square sections, were used in the calculations.

Moment of Inertia (I_x) of the Deformed Section—The deformations resulting from the rolling process reduce the moment of inertia of the section. The percentage reduction, ρ_i, in the moment of inertia I_x, can be described by

$$\rho_i\% = \frac{I_x - I_{\text{reduced}}}{I_x} \times 100 \tag{5}$$

Table 1. Comparison Between the Measured and Estimated Values for ρ_b, ρ_e and ρ_i

Member Size			Radius ft	ρ_b%		ρ_e%		ρ_i%	
h in.	*b* in.	*t* in.		Measured	Estimated*	Measured	Estimated**	Measured	Estimated***
4.0	2.0	0.1500	2.75	9.40	10.50	4.70	7.02	11.78	10.75
			4.00	6.25	7.81	3.15	3.94	8.81	7.91
			6.00	6.25	5.67	1.55	2.11	5.94	5.69
			8.00	4.70	4.51	0.25	1.35	2.96	4.50
4.0	2.0	0.2500	2.50	6.25	7.23	3.15	1.95	8.09	6.93
			3.00	4.70	6.26	2.35	1.47	5.57	5.98
			5.00	3.15	4.18	1.55	.67	0.00	3.94
			7.00	3.15	3.20	1.55	.40	0.00	2.99
4.0	2.0	0.3125	1.67	6.25	8.09	1.55	1.73	5.09	6.60
			2.17	6.25	6.58	1.55	1.15	4.54	5.33
			3.50	4.70	4.51	0.25	.55	1.90	3.61
			5.00	4.70	3.40	0.25	.32	0.00	2.70
4.0	3.0	0.1875	3.00	6.27	7.88	6.27	7.01	13.73	16.18
			4.00	5.20	6.27	4.17	4.50	10.67	12.79
			5.00	5.20	5.26	3.63	3.19	8.22	10.66
			8.00	3.13	3.63	1.03	1.54	5.88	7.27
4.0	3.0	0.2500	3.75	8.33	4.95	3.13	2.30	12.87	11.00
			5.00	3.63	3.94	2.10	1.48	7.94	8.70
			7.00	2.10	3.02	1.03	.88	7.43	6.61
			8.00	2.10	2.72	1.03	.71	4.93	5.93
4.0	4.0	0.1875	5.00	8.60	6.47	9.88	6.35	27.09	17.40
			8.00	5.10	4.46	7.02	3.08	19.70	11.86
			12.00	4.70	3.24	1.57	1.65	6.48	8.52
			16.00	3.12	2.58	0.77	1.06	5.93	6.74
4.0	4.0	0.3750	2.17	7.82	5.67	3.13	3.21	24.97	19.75
			3.00	3.12	4.39	2.72	1.95	13.57	15.16
			4.50	2.35	3.18	0.77	1.04	9.67	10.89
			9.00	1.57	1.84	0.12	.36	5.75	6.19
5.0	3.0	0.2500	3.00	13.53	10.29	6.27	7.10	20.06	17.25
			3.75	10.43	8.62	6.27	5.03	16.28	14.38
			6.00	6.27	5.94	1.57	2.44	8.28	9.80
			8.00	4.17	4.73	1.03	1.56	7.35	7.75
5.0	3.0	0.3750	3.00	9.37	7.06	2.63	2.17	17.26	10.87
			4.00	6.80	5.63	2.10	1.39	10.85	8.60
			5.50	4.70	4.37	1.03	0.85	9.08	6.63
			8.00	4.17	3.25	0.17	0.48	7.62	4.89
5.0	5.0	0.1880	4.50	11.26	12.02	25.0	23.52	47.87	34.36
			10.00	8.76	6.39	10.0	6.86	26.91	17.91
			12.00	6.26	5.53	8.76	5.18	22.50	15.43
			14.00	5.00	4.90	3.76	4.09	11.46	13.61
5.0	5.0	0.3750	4.50	7.50	6.52	4.38	4.51	24.78	25.65
			5.00	5.62	6.00	3.12	3.83	23.61	23.54
			8.00	2.50	4.13	2.50	1.85	19.22	16.04
			14.00	2.50	2.65	0.62	.78	11.46	10.16
6.0	4.0	0.1880	8.00	14.07	8.83	7.82	9.59	20.12	18.01
			12.00	10.95	6.41	4.70	5.13	17.79	12.94
			20.00	6.25	4.28	2.72	2.33	9.94	8.53
6.0	4.0	0.3750	4.00	13.27	9.98	3.90	5.88	22.18	22.46
			5.00	12.50	8.37	3.13	4.17	22.39	18.72
			8.00	7.02	5.77	2.72	2.02	13.71	12.76
			12.00	3.90	4.19	1.57	1.08	8.82	9.17

*, **, ***, Based on Eqs. 3, 4 and 6, respectively.

Table 1. (continued)

Member Size			Radius ft	$\rho_b\%$		$\rho_e\%$		$\rho_i\%$	
h in.	b in.	t in.		Measured	Estimated*	Measured	Estimated**	Measured	Estimated***
6.0	6.0	0.2500	8.00	7.30	9.31	11.98	12.83	24.60	31.55
			12.00	6.25	6.75	10.42	6.86	21.26	22.66
			14.00	6.25	5.98	6.25	5.41	19.35	19.98
			16.00	4.95	5.38	4.17	4.40	15.91	17.92
7.0	5.0	0.1880	8.00	7.50	11.88	13.76	21.82	18.78	28.48
			15.00	6.26	7.22	7.50	8.27	15.04	17.05
			24.00	5.62	4.98	3.76	4.01	10.90	11.62
			45.00	0.0	3.03	1.26	1.52	5.51	6.96
7.0	5.0	0.2500	8.00	7.50	10.31	8.76	12.58	15.31	27.18
			14.00	7.50	6.62	5.00	5.31	12.05	17.22
			22.00	5.00	4.63	2.50	2.64	10.59	11.91
			36.00	2.50	3.13	2.18	1.24	6.95	7.97
7.0	7.0	0.1880	24.00	6.26	6.54	16.07	8.57	27.89	18.73
			36.00	4.47	4.75	3.57	4.59	13.83	13.46
			60.00	3.13	3.17	1.34	2.09	7.87	8.87
			65.00	1.79	2.97	0.90	1.84	7.11	8.31
7.0	7.0	0.3120	8.00	6.25	11.15	11.61	16.92	26.51	43.72
			24.00	5.13	4.68	4.47	3.11	18.30	17.84
			36.00	4.47	3.39	2.23	1.66	14.18	12.82
			50.00	2.23	2.62	1.56	1.00	7.16	9.80
8.0	4.0	0.1880	16.00	7.82	8.31	10.97	7.41	17.00	13.77
			27.00	7.82	5.49	7.82	3.31	11.05	8.98
			40.00	5.47	4.02	1.57	1.80	6.96	6.52
			50.00	3.12	3.37	1.57	1.28	6.23	5.43
8.0	4.0	0.2500	8.00	10.95	13.91	13.27	13.07	20.02	22.25
			12.00	9.37	10.09	7.02	6.99	16.26	15.98
			18.00	7.82	7.32	2.72	3.74	11.12	11.48
			45.00	1.57	3.55	1.57	.91	8.67	5.43
8.0	4.0	0.3750	8.00	10.95	11.79	3.13	5.53	15.25	18.02
			12.00	9.37	8.55	2.72	2.96	12.82	12.94
			15.00	7.82	7.17	2.35	2.10	10.88	10.79
			20.00	5.10	5.71	1.57	1.35	9.31	8.53
8.0	8.0	0.2500	30.00	5.47	6.11	10.16	6.55	24.34	20.92
			45.00	4.89	4.43	6.25	3.51	19.78	15.03
			60.00	3.91	3.53	1.56	2.25	10.33	11.89
			80.00	3.12	2.81	0.79	1.44	9.39	9.40
8.0	8.0	0.3750	24.00	5.47	5.54	2.74	4.06	23.15	23.93
			30.00	5.07	4.64	2.61	2.88	18.25	19.95
			36.00	4.89	4.02	2.35	2.17	15.91	17.19
			45.00	3.91	3.37	1.17	1.54	14.31	14.33
10.0	6.0	0.2500	36.00	7.30	5.97	12.50	4.63	20.96	14.46
			50.00	7.30	4.61	10.42	2.79	17.72	11.06
			80.00	6.25	3.96	4.17	1.50	11.77	7.02
			100.00	6.25	3.32	1.57	1.06	10.61	5.85
10.0	6.0	0.3750	24.00	8.33	7.05	2.60	3.99	19.90	18.26
			36.00	8.33	5.11	2.08	2.14	16.94	13.12
			45.00	8.33	4.52	2.08	1.55	16.56	10.75
			55.00	8.33	3.85	1.05	1.14	14.72	9.13
10.0	10.0	0.2500	50.00	7.50	6.53	12.81	8.40	29.81	22.70
			80.00	7.19	4.50	13.13	4.07	31.16	15.47
			100.00	6.25	3.77	6.25	2.88	25.53	12.89
			120.00	6.25	3.27	5.00	2.18	19.16	11.11
10.0	10.0	0.3750	36.00	7.50	6.50	5.00	6.23	30.49	28.70
			45.00	7.50	5.45	3.75	4.42	26.60	23.92
			60.00	5.63	4.34	2.56	2.83	23.18	18.92
			100.00	5.63	2.90	1.88	1.29	16.61	12.47

*, **, ***, Based on Eqs. 3, 4 and 6, respectively.

Table 2. Coefficient of Variation V for Different Variables

Variable	V
t	0.0235
h or b	0.0020
R	0.0010*
(For rectangular sections)	
I_x	0.0311
I_y	0.0320
(For square sections)	
I_x	0.0330

*Assumed

where $I_{reduced}$ is the moment of inertia of the deformed section.

Values of ρ_i for all the tested specimens are listed in Table 1. Based on these values the following regression equation was derived to estimate the reduction in the moment of inertia for HSS members when bent to any radius, R:

$$\rho_i\% = (97.646)\,(R)^{-0.816}\,(h)^{-1.894}\,(b)^{-6.922}\,(t)^{-3.118}\,(I_x)^{-0.162}\,(I_y)^{3.692} \quad (6)$$

The multiple correlation coefficient and the standard error for Eq. 6 are 0.91 and 0.11%, respectively. A comparison between the actual values for ρ_i and those estimated by Eq. 6 is also given in Table 1. Based on the measured values of ρ_i given in Table 1, thirty-six specimens expressed reduction in the moment of inertia of less than 10%; while 47 specimens showed reductions between 10% and 20%, and the remaining 25 specimens exhibited reductions of more than 20%.

Parametric Study—From the above discussion it is clear that the magnitude of the cross-section distortions is a function of the geometry of the cross-section; and, the ratios between the depth h, the width b and the thickness t of the cross section have a significant influence on the resulting distortion. Therefore, a parametric study was undertaken on a series of HSS members, bent to the same radius of bend, and having various dimension ratios. The relations between h/t and the two parameters ρ_b and ρ_e describing the deformations of the web and the compression flange, respectively, are shown in Fig. 5. It is clear that as h/t increases both the deformations of the flange and the web increase. Similar relations not shown here for brevity, are found when the ratio b/t increases. The deformations of the flange and web also increase with increase in either the width b or the depth h of the cross section as shown in Fig. 6.

SUMMARY AND CONCLUSIONS

An experimental study was conducted to determine the relationships between the distortions in the cross-section of cold-bent HSS members, the geometry of the cross section and the radius of bend. Regression equations were derived establishing these relationships. Results show that cold-

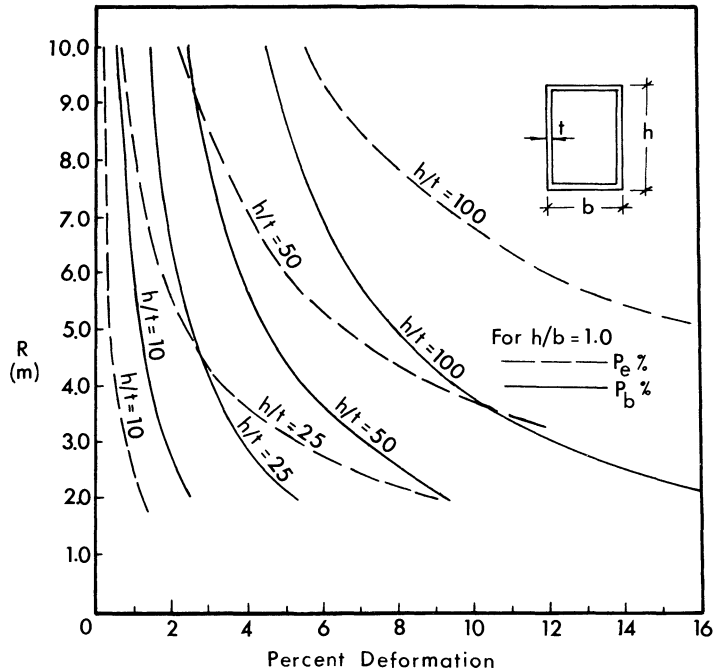

Fig. 5. Variation in cross-section deformation with changes in wall thickness of HSS

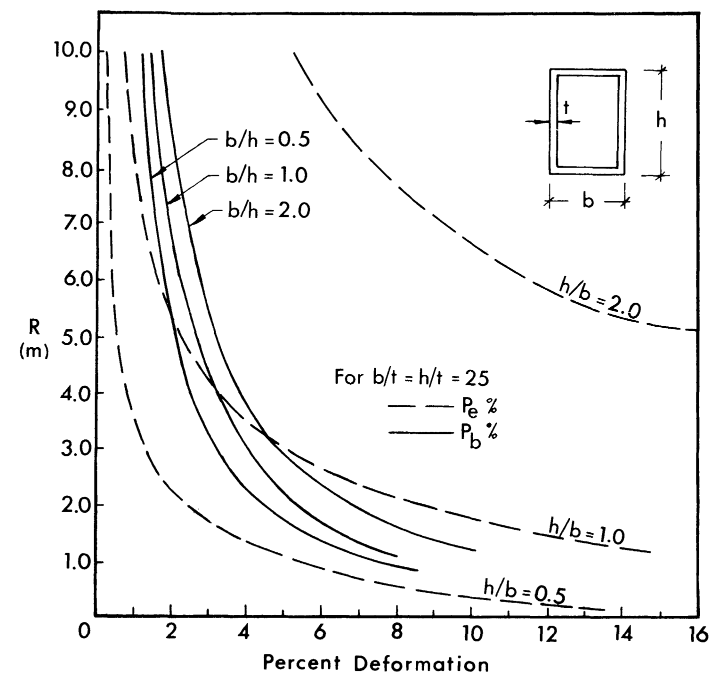

Fig. 6. Variation in cross-section deformation with changes in depth or width of HSS

bending of HSS members produces large permanent deformations in the cross-section. The magnitude of these deformations increases with decrease in the wall thickness of the cross section, with increase in the depth or width of the cross section, as well as with decrease in the imposed radius of bend. Generally the permanent distortions in the cross-section will effect a reduction of less than 20% in the moment of inertia before cold-bending.

ACKNOWLEDGEMENTS

The financial assistance provided by CIDECT through the Steel Company of Canada (STELCO) and from the Natural Sciences and Engineering Research Council under Grant No. A-1896, is appreciated. Thanks are also due to Hodgson's Steel and Iron Works, of Niagara Falls, Canada, for the use of their facilities to carry out the test program.

REFERENCES

1. *Ali, M. A. G.* Performance Factors for Steel Building Beams and Columns *M.A. Sc. Thesis, 1978, University of Windsor, Windsor, Ontario, Canada.*
2. *Brady, J. F.* Determination of Minimum Radii for Cold-bending of Square and Rectangular Hollow Structural Sections *CIDECT Programme 11B, May 1978, Final Report.*
3. *Kennedy, J. B. and A. M. Neville* Basic Statistical Methods for Engineers and Scientists *2nd Ed., Harper and Row Co., 1976, New York, N.Y.*
4. *Seddeik, M. M.* Deformations of Hollow Structural Beams Subjected to Cold-bending. *Ph.D. Thesis, 1985, University of Windsor, Windsor, Ontario, Canada.*